Journal of Engineering Physics and Thermophysics, Vol. 76, No. 1, 2003

NUMERICAL ANALYSIS OF THE INFLUENCE OF THE DEPTH OF A SPHERICAL HOLE ON A PLANE WALL ON TURBULENT HEAT EXCHANGE

S. A. Isaev,[a] A. I. Leont'ev,[b]
P. A. Baranov,[a] and I. A. Pyshnyi[b]

UDC 532.517.4:536.24

A numerical investigation of the influence of the depth of a spherical hole on a plane wall on vortex heat exchange has been carried out within the framework of the multiblock approach to solution of the steady-state Reynolds equations closed with the help of Menter's zonal model of shear-stress transfer and the energy equation.

1. One promising trend in the development of modern thermal physics is related to the vortex intensification of heat-exchange processes in the case of flow around the reliefs of holes. In the last two decades, thermophysical and hydroaerodynamic investigations have been carried out in a number of Russian scientific and production centers, with the result that prototypes and a number of commercial highly efficient power-engineering devices employing self-organization of tornado-like secondary jets in flows of gases and liquids have been designed. This phenomenon was found and studied roughly in the period from 1976 to 1988 in the pioneering works of the I. V. Kurchatov Institute of Atomic Energy [1]. They were further developed at the "BASÉRT" Russian Company, which owns the rights to the technologies of tornado energy exchange [2]. In the investigations carried out (see also [3]), large-scale vortex structures and their ensembles self-organizing in flows of gases and liquids near the energy-exchange surfaces which are formed by the relief of three-dimensional concavities-holes have been visualized and described for the first time. The intensification of the processes of heat and mass exchange and the hydrodynamic drag of isothermal and heated surfaces having such reliefs have been evaluated. A unique relation between the rate of removal of heat and the hydroaerodynamic loss in fluxes of energy carriers, which breaks the usual Reynolds analogy in favor of heat transfer, has been found.

The experience of investigations in this field (see, for example, [3–10]) suggests that the intensity of hydroaerodynamic processes in the case of flow around holes depends on many parameters determining the properties and regimes of the moving medium, the shape, size, and density of the elements of a relief on the surface in flow, the characteristics of the energy-exchange channel, and others. At the present time, these relations have been revealed only qualitatively in experiments with the simplest reliefs of three-dimensional concavities — holes of spherical shape, which is inadequate to establish and generalize the regularities of energy-exchange processes in self-organization of tornado-like vortices. Therefore, selection of three-dimensional concave reliefs, manufacture of specimens for extending and systematizing experimental investigations in this field, study of the structure of secondary tornado-like jets, and development of models of interaction of the flows of a viscous continuous medium with the reliefs of three-dimensional concavities are still considered to be the main problems.

Analysis of a number of recent experimental works [8–10] lends credence to the appeal of the considered method of vortex intensification of heat-and-mass-exchange processes (for cooling of devices of various purposes, among other things.) However, the widening of the geography of investigations and the increase in the number of publications have not yet led to the elucidation of the essence of controlling physical mechanisms. The experimental methods used for their analysis turned out to be limited to a certain extent because of the great number of influencing factors and since they are unable to disclose the structural features of three-dimensional vortex flows in great depth and in full measure. Therefore, preference in investigating the essence of the problem is given to numerical experiments carried out with the use of computer simulation complexes.

---

[a]Academy of Civil Aviation, St. Petersburg, Russia; email: isaev@SI3612.spb.edu; [b]N. É. Bauman Moscow State Technical University, Moscow, Russia. Translated from Inzhenerno-Fizicheskii Zhurnal, Vol. 76, No. 1, pp. 52–59, January–February, 2003. Original article submitted July 8, 2002.

The present work continues the cycle of investigations in the field of numerical simulation of convective heat exchange in turbulent flow of an incompressible fluid around an isolated spherical hole on a plane in a wide range of variation of the hole depth. The emphasis is on the analysis of the interrelation between the transformation of self-organizing vortex structures and the intensification of heat exchange in the neighborhood of the hole.

2. The preliminary numerical investigations of three-dimensional vortex flow and heat exchange in the neighborhood of a spherical hole on a plane have been carried out on the basis of calculations on multiblock H- and O-type grids within the framework of a strategy which is based on the splitting by physical processes and described in detail in [11]. For the turbulent regime [12, 13], they were carried out with the use of fairly coarse rectangular grids and the high-Reynolds k–ε model of Launder and Spalding. The reproduction of a vortex structure in laminar separated flow around a deep hole has been substantially refined with the use of cylindrical grids [14], but in this case researchers faced insurmountable difficulties in calculating turbulent flows in the process of simulation of the near-axis singularities.

A significant amount of progress in numerical simulation of convective heat exchange in the neighborhood of isolated holes has been attained owing to the development of multiblock computational technologies [15] and the application of the zonal low-Reynolds k–ω model of shear-stress transfer (SST) proposed by Menter [16]. Noteworthy is a substantial refinement of the numerical predictions and a more rational employment of computational resources, which predetermines the improved quality of the numerical experiment. In [17], it has been found that the structure of the turbulent vortex pattern in an asymmetric hole is transformed; this is due to the passage from the generation of two vortex cells within the hole to a single-tornado structure. The bifurcation of the vortex pattern in a deep spherical hole in the case of turbulent flow around it has been demonstrated in [18], and the interrelation between the transformation of the vortex structure and the intensification of heat exchange within the hole has been pointed out for the first time. In [19, 20], a verification of the computational multiblock algorithm has been made on the basis of a comparative analysis of the results of numerical and physical simulation concerning the vortex structure of laminar flow [19] and the distributions of the local and integral coefficients of heat transfer in the turbulent regime [20]. In [19], the influence of the depth of a hole on the vortex dynamics has also been analyzed for the case of laminar flow past a plane with a hole.

3. In the present work, we solve the problem of turbulent convective heat exchange for three-dimensional vortex flow of an incompressible viscous fluid in the neighborhood of an isolated spherical hole on a plane. The heat problem and the dynamic problem are considered individually, i.e., the energy equation is solved for the fields of velocity and characteristics of turbulence calculated in advance.

The calculation of stationary turbulent vortex flow in the neighborhood of a hole is based on the widely accepted concept of splitting by physical processes applied to solution of the Reynolds-averaged Navier–Stokes equations which are closed using Menter’s model of shear-stress transfer. The concept is realized in the process of global iterations involving the known SIMPLEC procedure of pressure correction. The indicated two-stage procedure of the "predictor–corrector" type is meant for determining the Cartesian components of the velocity and the pressure for frozen fields of vortex viscosity and characteristics of turbulence.

The original features of the finite-volume algorithm developed are as follows: a) the initial equations are written in increments of dependent variables, b) the convective terms on the explicit side are approximated by the upwind Leonard scheme with quadratic interpolation, c) the convective terms on the implicit side are approximated by the upwind scheme with one-sided differences, d) artificial diffusion is introduced into the implicit side for damping high-frequency oscillations, e) the Rhee–Chou monotonizer is used in the pressure-correction block because of the centered computational template with an empirically determined coefficient of 0.1, and f) the difference equations are solved by the method of incomplete matrix factorization.

In the global iterative process, local iterations on solution of the equations for the characteristics of turbulence are carried out at each stage.

It should be emphasized that the computational methodology in such a form developed for monoblock grids was approved in the late 1980s—early 1990s and described in detail in [11]. The construction of a multiblock algorithm in turn is associated with numerical simulation of flows in multiply connected regions within the framework of the approach based on the decomposition of the computational region of complex geometry into fragments and the use of intersecting grids of simple topology. In the two-dimensional variant, the algorithm has been applied to calculation of flow around bodies with vortex cells [15]. A generalization of the multiblock technique to the case of three-dimensional separated flows has been made with the example of simulation of an air flow in a channel with a circular cavity [21], in predicting the smoke content in the rooms of an underground transportation system and for solution of the problem on flow around an isolated hole on the plane [17–20].

Multiblock structurized grids are considered to be topologically independent, i.e., generated without the fulfillment of any coordinating conditions. The grid cells are divided into computational cells and connected cells.

The computational cells are those cells in which the equations are solved. In all the other cells the sources are assumed to be zero and the coefficients (except a_{p} [11], which is equal to unity) are also zero. Therefore, the calculation is carried out by the direct method over the entire region. For the bounds of the computational cells, coincident with the outer boundary of the region or with the boundary of the body, an additional memory is provided for storage of metric coefficients and dependent variables. On all the other bounds, the values are determined by interpolation [19]. On the side of these bounds a computational cell should have at least two neighbors to provide the second order of approximation of the convective terms.

The connected cells are those cells the values of the parameters in which are determined by a nonconservative linear interpolation of data from other subregions. Unfortunately, the use of the dependences of second order has not met with success, since oscillations appeared in the zones of large gradients of the determining parameters.

Connected cells can conditionally be divided into two groups — the cells that are set compulsorily (they are, as a rule, peripheral layers of the inner grids) and those that are set to be such in the process of generation of grids. The division is conditional and is determined by only the method of setting. They are identical algorithmically.

Prior to solving each equation, the values of the variables in the connected cells are determined. This does not take much time since the interpolation coefficients are calculated in advance. Then, one iteration step is made in each region. The sequence of scanning of the regions is of no importance. In passage to the next iteration (not the global iteration but the iteration for this equation), the values of the corrections for a given variable are determined. It is of no importance for the momentum equation since only one iteration is made as a rule. For the majority of other variables, the absence of this step slows down convergence only slightly. It is only for the pressure that account for the corrections taken from other regions is crucial since this is a unique mechanism which makes it possible to determine this constant automatically with an accuracy to which the pressure is determined.

For description of flow and heat exchange in the neighborhood of holes we introduce the following grids (see Fig. 1):

A. *Outer rectangular grid*. It is used for simulation of near-wall flow, and in the case where holes are absent it is a unique grid for solving the problem.

B. *Additional rectangular grid*. It is inner relative to the outer grid and is used for a more comprehensive description of the neighborhoods of the hole arrangement.

C. *Cylindrical grid*. It discretizes the space in the neighborhood of the spherical hole.

D. *Rectangular grid*. It is a "patch" on the axis of the cylindrical grid.

E. *Rectangular grid for a more comprehensive description of the near wake of the hole*. It is expedient to use it for isolated holes. It will suffice to use grid B for packets of holes.

For all the grids except the outer grid, two layers of peripheral cells are set to be connected. They are side and upper layers. For grid C, two inner cylindrical layers are added. Then, the following procedure is carried out in preparation of the initial information. The intersection of each grid and all the other grids that are wholly or partially inside it is checked. In the case of holes, the intersection of each grid and all the grids in the list is checked. A cell of a grid, which has found itself within the grid of the next level, is marked as suitable for being connected, but interpolation is not performed yet and the possibility of establishing a connection is only checked. Of course, the linear hierarchy can not always hold; therefore, for some holes the setting of one hole to be "guiding" and of another to be "guided" is determined only by the order of them in the program.

At the end of preparation, the calculation of connections for all the marked cells is carried out, i.e., interpolation polynomials are constructed. The search is made only among the computational cells and over all the regions. Therefore, for example, a cell of grid A marked as suitable for being connected in checking the intersection of it and grid B can turn out to be actually connected with any grid of the next level. This has been done intentionally to ensure that in the calculation the interpolated values are taken from the narrowest grids.

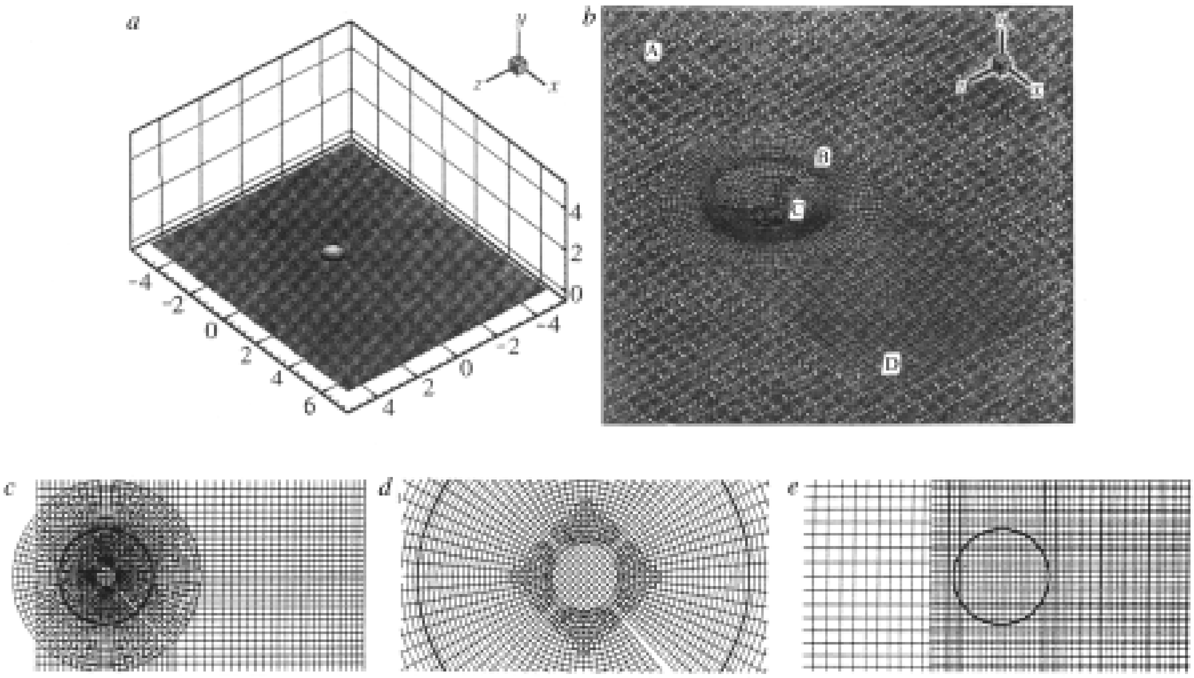

Fig. 1. Computational region (a) and fragments of a multiblock computational grid (b): [A) outer grid; B) cylindrical grid; C) "patch"; D) additional grid in the near wake], c) superposition of the cylindrical grid around the hole and the additional grid in the wake; d) fragment of the cylindrical grid around the hole and the "patch"; e) superposition on the outer rectangular grid in the channel of the additional grid in the wake with the applied contour of the hole.

A specific drawback of such an approach is an excessively large number of connected cells, which requires the increased use of random-access memory in the computer, whereas in actual practice all the connected cells that are at a distance of more than two indices from the computational cells can be omitted. But to do this, it is necessary to change the system of numbering of the cells and bring it into correspondence with that used for nonstructurized grids.

To stabilize the computational process a lower relaxation with coefficients for the velocity (0.5), the pressure (0.8), the characteristics of turbulence (0.5), and the vortex viscosity (0.35) is introduced at each iteration step.

In solving the steady-state energy equation, the general features of the computational algorithm are retained. We note that in this case the Prandtl number of the medium is taken to be 0.7 and the turbulent Prandtl number is taken to be 0.9.

4. A series of calculations of convective heat exchange in spherical holes with a rounded sharp edge (rounded radius 0.1), carried out for the given Reynolds number $\mathrm{Re} = 2.3 \cdot 10^4$ and the depth of the hole Δ varied from 0.03 to 0.2, is considered.

The computational region represents a curvilinear parallelepiped with the lower boundary coincident with the plane in flow on which a spherical hole is located (Fig. 1). At the inlet to the region, a uniform flow with a characteristic velocity U and a thickness of the boundary layer of 0.175 is set. Within the limits of the boundary layer, the longitudinal velocity component changes by the law 1/7, while the other velocity components and the excess pressure are taken to be equal to zero. The characteristics of turbulence at the inlet to the computational region correspond to the conditions of the physical experiment [20]; the degree of turbulence of the flow is set to be 1.5%. The adhesion conditions are set on the wall and the characteristics of turbulence in the near-wall zone are selected to be such as in [15]. At all the other boundaries, "soft" boundary conditions or, to put it otherwise, conditions of continuation of the solution are set. The diameter of the hole D is taken to be the dimensionless scale.

To obtain a solution of acceptable exactness four different-scale grids are introduced. The above-indicated computational region with dimensions $12 \times 5 \times 10$ is discretized using the outer grid which contains $55 \times 50 \times 40$ computational cells. The size of the near-wall step is selected to be 0.0008, and the minimum steps in the longitudinal

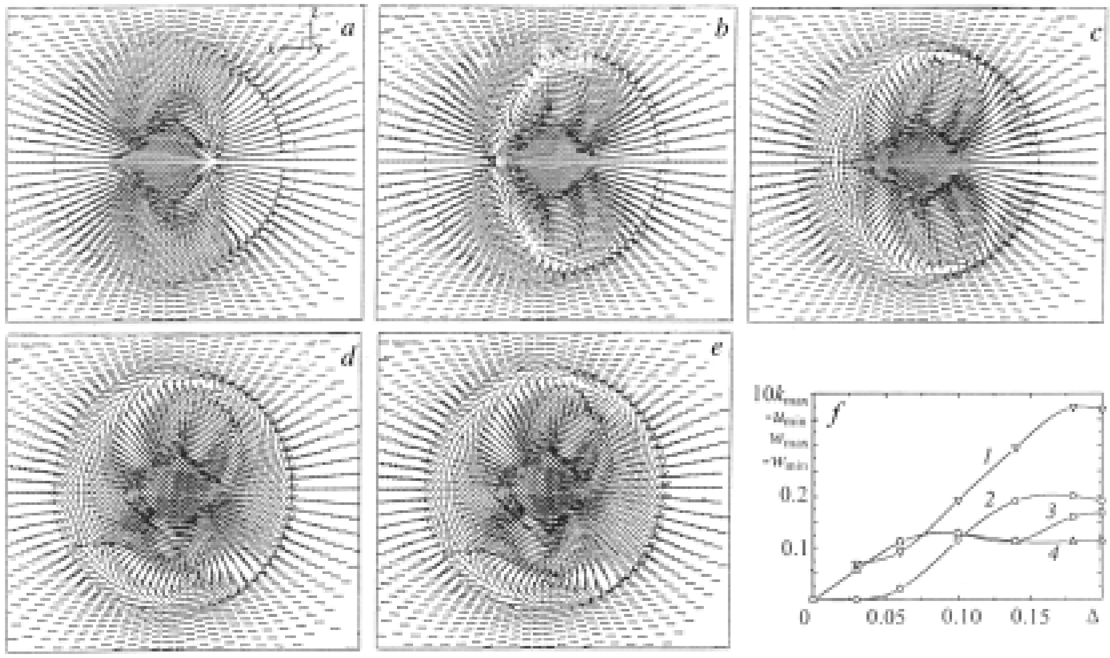

Fig. 2. Comparative analysis of the patterns of directions of the velocity vectors in the near-wall layer in the neighborhood of a spherical hole with a varying depth: 0.06 (a), 0.1 (b), 0.14 (c), 0.18 (d), and 0.2 (e), and dependences of the extremum and local characteristics of the vortex flow on Δ (f): k_{max} (1), $-u_{max}$ (2), w_{max} (3), and $-w_{max}$ (4).

and transverse directions are selected to be 0.15. The area of the spherical hole whose center with coordinates $x = z = 0$ is at a distance of 5 from the inlet boundary represents an annular cylindrical subregion of diameter 2 looming 0.175 above the plane. The indicated subregion is covered with a cylindrical grid matched with the curvilinear wall in flow and containing $40 \times 40 \times 80$ cells. For this grid the near-wall step is 0.0008 and the longitudinal step of the grid in the region of the sharp edge is 0.015. The radius of the inner ring is selected to be 0.1, and a uniform grid is constructed in the circumferential direction.

The cylindrical zone inside the ring is covered with a subregion in the form of a parallelepiped with a curvilinear base with dimensions of the square 0.5×0.5. The grid within this subregion is matched along the vertical coordinate with the adjacent cylindrical grid, and the base is divided into 12×12 uniformly distributed cells.

To provide the proper accuracy of calculation of the parameters within the hole and in the wake of it we introduce an additional computational subregion in the form of a parallelepiped with dimensions $3.5 \times 0.175 \times 2$ containing $55 \times 35 \times 30$ cells. The near-wall step is also equal to 0.0008 and the origin of the subregion is tied to the point with coordinates $x = -0.75$, $z = 0$.

5. Some of the results obtained are presented in Figs. 2–5.

Successive increase in the depth of a spherical hole leads to the transformation of the patterns of flow and the temperature fields in the surface layer. In passage from Δ = 0.03 to Δ = 0.06, the unseparated character of flow becomes separated. At Δ = 0.06, the zone in the neighborhood of the leeward slope of the hole is filled with a retarded, easily heated fluid. The last circumstance decreases the level of heat loads. The windward side of the hole is simultaneously the region of interaction of the separated shear layer in the incoming flow with the wall. The largest velocity gradients and heat fluxes are observed immediately behind the hole.

Even a small concavity in the wall, as has already been indicated in [12, 13], causes the effect of a "vacuum cleaner" in the near-wall region. For Δ = 0.06–0.1 the transverse velocities reach 10% of the velocity of the incoming flow. It is significant that the coefficient of heat transfer from the wall ($C = \mathrm{Nu}/\mathrm{Nu}_{pl}$) markedly decreases in the near wake behind the hole. At the same time, for the holes of small or moderate depth the degree of heat transfer depends on Δ weakly and it is close to the level of heat transfer from a smooth wall.

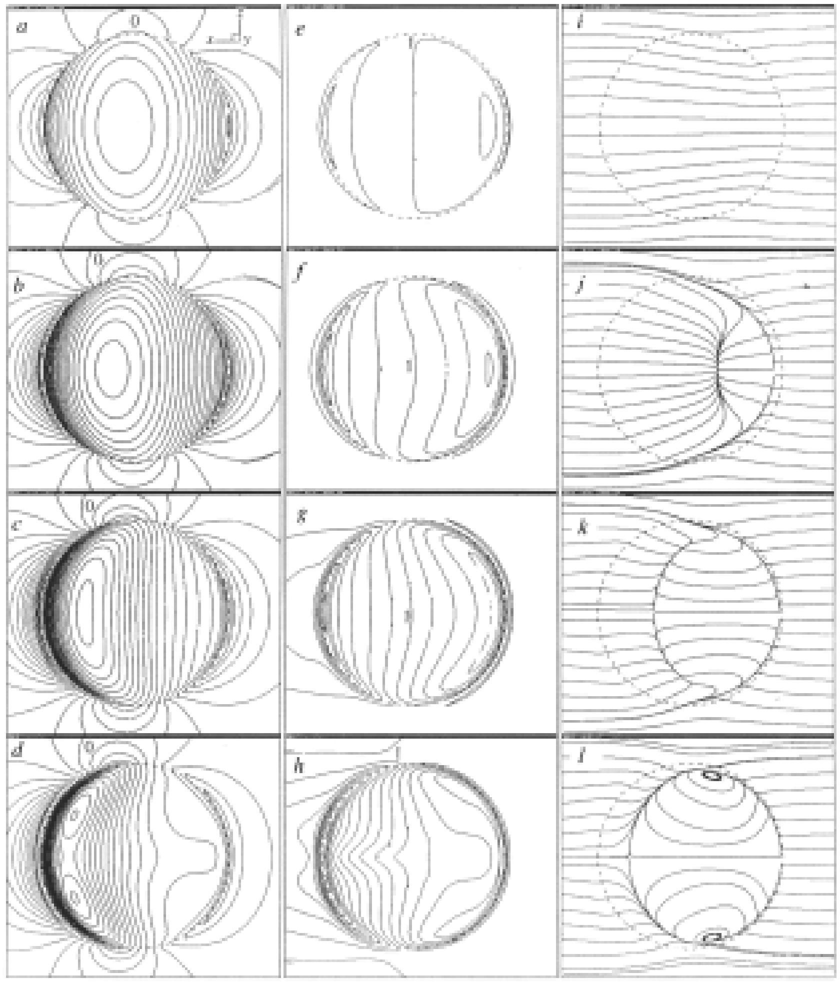

Fig. 3. Patterns of isobars distributed over the surface of the hole (a–d) and isotherms in the near-wall layer at a distance of 0.0004 from the wall (e–h) and patterns of spreading of the fluid on the surface of the hole (i–l): Δ = 0.03 (a, e, i), 0.06 (b, f, j), 0.1 (c, g, k), and 0.14 (d, h, l); 0) zero level of excess pressure, 1) temperature level $T = 97^{o}$C. The isobars are drawn with a step of 0.005 and the isotherms are drawn with a step of 0.5^{o}.

At Δ = 0.1, a quasi-two-dimensional separation zone is formed in the central region of the hole, and the separation line is practically coincident with the boundary of the spherical hole denoted by the dashed line in the figures. As the depth increases, the separation zone, as in the laminar regime [19], occupies an increasing region of the hole, and the maximum longitudinal velocity of reverse flow increases to values of the order of 20% of the velocity of the incoming flow.

Comprehensive analysis of the pattern of directions of the velocity vectors in Fig. 2b points to the existence of additional points of fluid spreading on the windward slope of the hole. The indicated two source-type singular points located approximately at an angle of 45^{o} to the direction to the center of the hole generate weak currents to the symmetry plane and to the periphery, where the fluid flows out of the hole as two branches. On the one hand (Fig. 5a), as has already been noted in [19], for a hole of moderate depth, similarly to flow around a wing of finite span, a Π-shaped vortex descends to the near wake, and on the other hand, in the central part of the hole there arise two fairly extended vortex rings disconnected in the neighborhood of the symmetry plane.

The passage to a deeper hole (Δ = 0.14) is accompanied by a marked change in the pattern of spreading. The almost double increase in the longitudinal component of the reverse flow is due to the disconnection of the separation

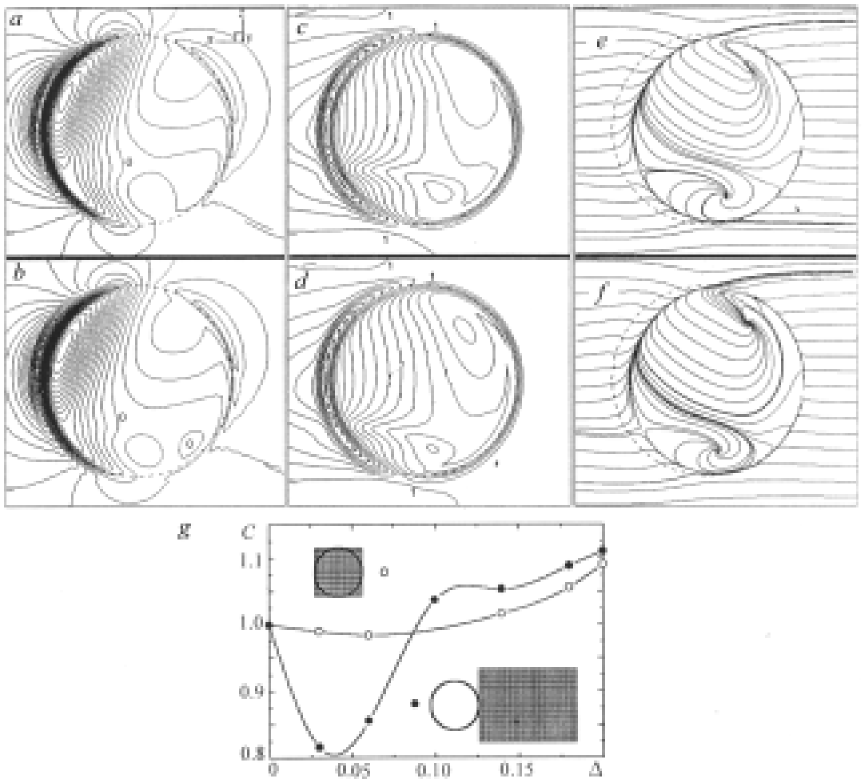

Fig. 4. Patterns of isobars distributed over the surface of the hole (a, b) and isotherms in the near-wall layer at a distance of 0.0004 from the wall (c, d), patterns of spreading of the fluid on the surface of the hole (e, f), and dependences of the coefficient of relative heat transfer C (g) on Δ: $\Delta = 0.18$ (a, c, e), 0.2 (b, d, f); 0) zero level of excess pressure, 1) temperature level $T = 97^{\circ}$C. The isobars are drawn with a step of 0.005 and the isotherms with a step of 0.5°.

zone in the peripheral side parts of the hole and the formation of two windows open to the incoming flow. As has already been noted in [20], on the side slopes of the hole there arise singular points of the type of focuses which, in their neighborhood, generate tornado-like jet counterflows transporting the fluid to the center of the hole. The intense spreading of the fluid in the symmetry plane transforms markedly the pressure field and the temperature field in the near-wall layer. It should be noted first of all that the distribution of the excess pressure on the windward slope of the hole is two-peak in character. Moreover, if at $\Delta = 0.1$ the pressure and the temperature in the transverse direction are practically constant near the symmetry plane of the hole, at $\Delta = 0.14$ we have a local extremum of the temperature at $z = 0$ throughout the hole and a local extremum of the pressure in its leeward part.

Such a character of distribution of the local force and heat characteristics in the hole is to a certain extent due to the three-dimensional vortex structure of flow (Fig. 5b). The pattern of flow around a spherical hole is symmetric, i.e., a two-cell vortex structure is realized in the hole. Just as for $\Delta = 0.1$, for $\Delta = 0.14$ the structures become disconnected in the neighborhood of the symmetry plane; vortex rings shifting to the center of the hole at $\Delta = 0.14$ are localized inside the vortex cocoons. Thus, in the neighborhood of the symmetry plane in the near-wall zone there arises flow analogous to the flow from the source.

In turbulent flow around nearly deep holes ($\Delta = 0.18$–0.2), the structure of vortex motion within them changes abruptly and becomes nonsymmetric. Along with the intensification of the transverse secondary flow progressing with increase in Δ (the maximum of the velocity approaches $0.2U$), it becomes dominating in one direction. Simultaneously, in the opposite direction, the transverse velocity decreases to a value equal approximately to $0.12U$ and ceases to depend on Δ.

Remaining open on one side relative to the incoming flow, the deep hole closes on the other side. In this case, one vortex cell within the hole actually disappears. As is evident from Fig. 5c, the transverse swirling flow

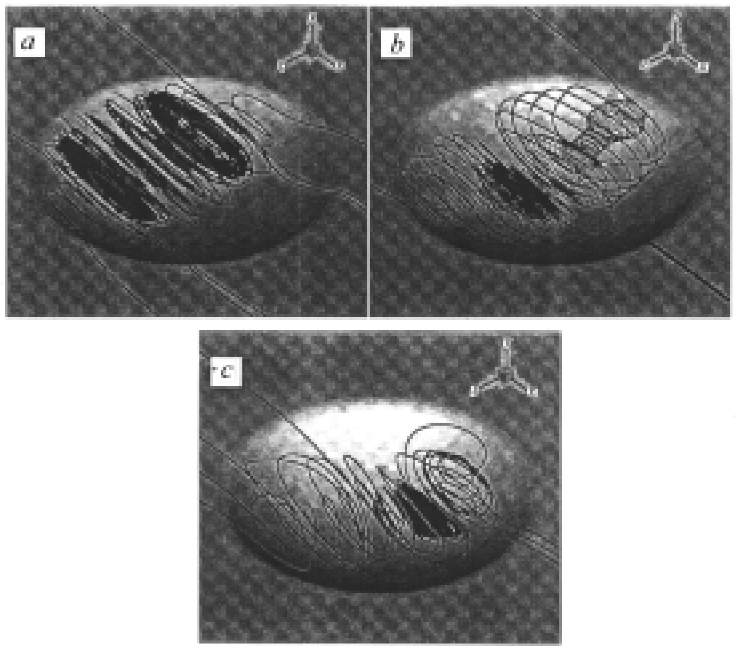

Fig. 5. Computer identification of the vortex structures in spherical holes: a) Δ = 0.1, b) 0.14, and c) 0.18.

leaves the hole at an angle close to 45^{o}. It should be pointed out that a vortex ring similar to the above-mentioned rings forms in the counterpressure zone.

As Δ increases, the generation of turbulence by the hole becomes more intense (Fig. 2f), which is in good agreement with the view of holes as elements of artificial roughness. The intensification of vortex flow in the hole in turn causes an increase in the heat transfer from the hole and its neighborhood.

For deep holes ($\Delta \sim 0.2$), the deformation of the layered temperature near-wall layer becomes marked in the neighborhood of the hole, which is due to the structural transformation and stimulates the heat transfer in this region. The last-mentioned circumstance confirmed, to a certain extent, the conclusions made in [18].

The authors express their thanks to R. Banker for useful discussions of the problem.

This work was carried out with financial support from the Russian Foundation for Basic Research (project Nos. 02-02-17562, 02-02-81035, and 02-01-01160).

NOTATION

x, y, z, Cartesian coordinates; U, velocity of the incoming flow; D, diameter of the hole; Δ, depth of the hole; u and w, longitudinal and transverse velocity components; k, energy of turbulent pulsations; ε, rate of dissipation of turbulent energy; ω, specific rate of dissipation of turbulent energy; T, temperature; a_p, total coefficient of the difference equations; Re, Reynolds number; Nu, Nusselt number; $C = \mathrm{Nu}/\mathrm{Nu}_{pl}$, coefficient of relative heat transfer of the singled-out element of the surface in flow. Subscripts: max and min, maximum and minimum values; pl, parameter on the wall; p, center of the cell.

REFERENCES

1. V. V. Alekseev, I. A. Gachechiladze, G. I. Kiknadze, et al., in: *Proc. 2nd Russ. Nat. Conf. on Heat Transfer*, Vol. 6, *Enhancement of Heat Transfer. Radiative and Combined Heat Transfer* [in Russian], Moscow (1998), pp. 33–42.
2. G. I. Kiknadze, I. A. Gachechiladze, and V. G. Oleinikov, *RF Patent No. 2020304* as of 30.09.1994.
3. M. Ya. Belen'kii, M. A. Gotovskii, B. M. Lekakh, et al., *Teplofiz. Vys. Temp.*, **29**, No. 6, 1142–1147 (1991).

4. V. N. Afanas’ev, A. I. Leont’ev, Ya. P. Chudnovskii, et al., *Hydrodynamics and Heat Transfer in the Case of Flow around Single Holes on an Initially Smooth Surface* [in Russian], Preprint No. 2–91 of Moscow State Technical University, Moscow (1990).
5. V. I. Terekhov, S. V. Kalinina, and Yu. M. Mshvidobadze, *Russ. J. Eng. Thermophys.*, **5**, 11–34 (1995).
6. N. Syred, A. Khalatov, A. Kozlov, et al., *Effect of Surface Curvature on Heat Transfer and Hydrodynamics within a Single Hemispherical Dimple*, ASME Paper, 2000-GT-236 (2000).
7. A. V. Shchukin, A. P. Kozlov, Ya. P. Chudnovskii, et al., *Izv. Akad. Nauk SSSR*, *Énergetika*, No. 3, 47–64 (1998).
8. M. K. Chuy, Y. Yu, H. Ding, J. P. Downs, et al., *Concavity Enhancement Heat Transfer in an Internal Cooling Passage*, ASME Paper, 97-GT-437 (1997).
9. H. K. Moon, T. O’Connell, and B. Glezer, *Channel Height Effect on Heat Transfer and Friction on a Dimpled Passage*, ASME Paper, 99-GT-163 (1999).
10. G. I. Mahmood, M. L. Hill, D. L. Nelson, et al., *Local Heat Transfer and Flow Structure on and above a Dimpled Surface in a Channel*, ASME Paper, 2000-GT-230 (2000).
11. I. A. Belov, S. A. Isaev, V. A. Korobkov, *Problems and Methods of Calculation of Separated Flows of an Incompressible Fluid* [in Russian], Leningrad (1989).
12. S. A. Isaev, A. I. Leont’ev, and A. E. Usachov, *Izv. Ross. Akad. Nauk*, *Énergetika*, No. 4, 140–148 (1996).
13. S. A. Isaev, A. I. Leont’ev, and A. E. Usachov, *Inzh.-Fiz. Zh.*, **71**, No. 3, 484–490 (1998).
14. S. A. Isaev, A. I. Leont’ev, A. E. Usachov, et al., *Izv. Ross. Akad. Nauk*, *Énergetika*, No. 2, 126–136 (1999).
15. A. V. Ermishin and S. A. Isaev (eds.), *Control over Flow past Bodies with Vortex Cells as Applied to Aircraft of Integral Arrangement* (*Numerical and Physical Modeling*) [in Russian], Moscow–St. Petersburg (2001).
16. F. R. Menter, *AIAA J.*, **32**, No. 8, 1598–1605 (1994).
17. S. A. Isaev, A. I. Leont’ev, and P. A. Baranov, *Pis’ma Zh. Tekh. Fiz.*, **26**, Issue 1, 28–35 (2000).
18. S. A. Isaev, A. I. Leont’ev, P. A. Baranov, et al., *Dokl. Ross. Akad. Nauk*, **373**, No. 5, 615–617 (2000).
19. S. A. Isaev, A. I. Leont’ev, P. A. Baranov, et al., *Inzh.-Fiz. Zh.*, **74**, No. 2, 62–67 (2001).
20. S. A. Isaev, A. I. Leont’ev, Kh. T. Metov, et al., *Inzh.-Fiz. Zh.*, **75**, No. 3, 53–59 (2002).
21. P. A. Baranov, S. V. Guvernyuk, M. A. Zubin, et al., *Izv. Ross. Akad. Nauk, Mekh. Zhidk. Gaza*, No. 5, 44–56 (2000).
22. P. A. Baranov, A. D. Golikov, S. A. Isaev, et al., in: *Proc. 3rd Int. Sem. on Fire and Explosion Hazards*, Prestow (2001), pp. 745–757.